

Degradation of alachlor and pyrimethanil by combined photo-Fenton and biological oxidation

M.M. Ballesteros Martín^{a,*}, J.A. Sánchez Pérez^a, J.L. García Sánchez^a,
L. Montes de Oca^a, J.L. Casas López^a, I. Oller^b, S. Malato Rodríguez^b

^a Departamento de Ingeniería Química, Universidad de Almería, 04120 Almería, Spain

^b Plataforma Solar de Almería-CIEMAT, Carretera de Senés km 4, 04200 Tabernas, Almería, Spain

Received 28 September 2007; received in revised form 15 November 2007; accepted 20 November 2007

Available online 23 November 2007

Abstract

Biodegradability of aqueous solutions of the herbicide alachlor and the fungicide pyrimethanil, partly treated by photo-Fenton, and the effect of photoreaction intermediates on growth and DOC removal kinetics of the bacteria *Pseudomonas putida* CECT 324 are demonstrated. Toxicity of 30–120 mg L⁻¹ alachlor and pyrimethanil has been assayed in *P. putida*. The biodegradability of photocatalytic intermediates found at different photo-treatment times was evaluated for each pesticide. At a selected time during batch-mode phototreatment, larger-scale biodegradation kinetics were analysed in a 12 L bubble column bioreactor. Both alachlor and pyrimethanil are non-toxic for *P. putida* CECT 324 at the test concentrations, but they are not biodegradable. A ~100 min photo-Fenton pre-treatment was enough to enhance biodegradability, the biological oxidation response being dependent on the pesticide tested. The different alachlor and pyrimethanil respiration and carbon uptake rates in pre-treated solutions are related to change in the growth kinetics of *P. putida*. Reproducible results have shown that *P. putida* could be a suitable microorganism for determining photo-Fenton pre-treatment time.

© 2007 Elsevier B.V. All rights reserved.

Keywords: Alachlor; Pyrimethanil; Photo-Fenton; Biodegradability; *Pseudomonas putida*

1. Introduction

Because human activities have an increasing impact on the ecosystem, natural resource management strategies based on sustainable and integrated development must be implemented. The Plan of Implementation of the World Summit on Sustainable Development adopted in Johannesburg [1], includes actions at all levels, e.g., introduction of affordable sanitation and industrial and domestic wastewater treatment technologies. In order to achieve the goals for bodies of surface water, the European Commission has adopted the Water Framework Directive [2] to progressively eliminate major pollutants. Alachlor is one of the 33 EU priority substances listed in the Commission proposal (COM(2006)397 final) setting environmental quality standards for surface waters (http://ec.europa.eu/environment/water/water-framework/priority_substances.htm),

while pyrimethanil is included in the Commission Directive 2006/74/CE list of authorised and evaluated substances.

Alachlor, 2-chloro-2',6'-diethyl-N-methoxymethyl acetanilide, is a common agricultural herbicide. Alachlor causes cancer in laboratory animals and its mutagenicity has been demonstrated [3]. In addition, alachlor has toxic and genotoxic effects [4], and could also contribute to infertility [5]. Pyrimethanil, N-(4,6-dimethylpyrimidin-2-yl)-aniline is an anilino-pyrimidine restricted to use as fungicide in agriculture. Although available studies show no evidence of mutagenic, genotoxic or carcinogenic potential of pyrimethanil, an increase in liver weight accompanied by histopathological changes in liver and thyroid have been observed in short-term toxicity studies in rats and mice [6].

A variety of effective treatment techniques for wastewater containing alachlor or pyrimethanil are available [7–10]. Among them, advanced oxidation processes (AOPs) may become the most extensively used for these pesticides not treatable by conventional techniques due to their high chemical stability and/or low biodegradability. Of the solar AOPs, photo-Fenton has been

* Corresponding author.

E-mail address: mmenta@ual.es (M.M. Ballesteros Martín).

Nomenclature

DOC_i	initial DOC concentration given by photoreaction intermediates (mg L^{-1})
DOC_f	DOC concentration measured at the end of culture (mg L^{-1})
DOC_m	minimum concentration that cannot be metabolized by the cells (mg L^{-1})
J	objective function (dimensionless)
K_S	saturation constant (mg L^{-1})
K_I	inhibition constant (mg L^{-1})
r_S	carbon uptake rate ($\text{mg L}^{-1} \text{h}^{-1}$)
S	substrate (DOC) concentration (mg L^{-1})
t_{30W}	normalized illumination time (h)
UV	average solar ultraviolet radiation (W m^{-2})
V_T	total volume of water loaded in the pilot plant (L)
V_i	total irradiated volume (L)
X	biomass concentration (mg L^{-1})
$X(i)_{\text{mod}}$	simulated state space vector (mg L^{-1})
$X(i)_{\text{exp}}$	experimental state space vector (mg L^{-1})
$Y_{X/S}$	yield coefficient on substrate (g g^{-1})

Greek letters

μ	specific growth rate (h^{-1})
μ_{max}	maximum specific growth rate (h^{-1})

demonstrated to be more effective than TiO_2 [11–15]. Nevertheless its cost [14–16] for total oxidation of hazardous organic compounds remains high compared to those of biological treatment. However, their use as a pre-treatment for biodegradability enhancement of wastewater containing recalcitrant compounds can be justified if the intermediates resulting from the reaction are more biodegradable than the parent compounds and can therefore be quickly degraded by biological treatment [17,18]. Thus, photochemical pre-treatment can be shortened when combined with biological oxidation. Nonetheless, photocatalytic degradation products could be as or even more toxic and recalcitrant than the original pollutant, so the biodegradability of the mixture of intermediates formed as the chemical reaction proceeds must be evaluated as a function of photo-treatment intensity.

There are many publications dealing with integrated chemical and biological oxidation processes for wastewater for a variety of single compounds (e.g., aromatics, pesticides, etc.) [19–21] and multicomponent feed streams as industrial wastewater and landfill leachate [22–24]. Coupling chemical pre-oxidation with biological post-treatment is conceptually beneficial as it can lead to increased overall treatment efficiencies compared with the efficiency of each individual stage [22]. Thus, for the treatment of complex mixture of effluents hybrid treatments appear to be the need for the future [23]. Despite the prevalence of examples evident in these reviews kinetic models are not widely available as a method of analysis [25].

This paper reports on a study of the biodegradability of aqueous alachlor and pyrimethanil solutions treated by photo-Fenton

at the point when changes are caused in pure bacteria growth kinetics by photoreaction intermediates. Synthetic wastewater made from a mixture of biodegradable organic compounds and the test substances (pesticides or photo-degradation intermediates) was used to assess the biodegradability of alachlor and pyrimethanil as well as the photo-treated solutions. The bacteria *P. putida* CECT 324 was selected as a model microorganism [26] to evaluate biodegradability, and changes observed in growth and degradation kinetics caused by the test substances were compared to the baseline given by a biodegradable C-source.

P. putida sensitivity to toxicity of alachlor and pyrimethanil was first assayed in a 30–120 mg L^{-1} concentration range. Then the biodegradability of the photocatalytic intermediates from each pesticide was evaluated in Erlenmeyer flasks as a function of a normalized photo-treatment time (t_{30W}) that characterizes the progress of the photo-Fenton process. The kinetics of larger-scale batch-mode biodegradation was analysed in a 12 L bubble column bioreactor at a selected photo-treatment time. The final goal of the paper is to propose a consistent and reproducible method for assessing biodegradability using a model microorganism, as an alternative to other methods based on activated sludge.

2. Materials and methods

2.1. Chemicals

Technical-grade alachlor (2-chloro-2',6'-diethyl-N-methoxymethylacetanilide, 95%, Aragonas Agro S.A.) and pyrimethanil (98.2% technical grade $\text{C}_{12}\text{H}_{13}\text{N}_3$, Agrevo S.A.) were used as received. Distilled water used in the pilot plant was supplied by the Plataforma Solar de Almería distillation plant (conductivity $< 10 \mu\text{S cm}^{-1}$, $\text{Cl}^- = 0.7\text{--}0.8 \text{ mg L}^{-1}$, $\text{NO}_3^- = 0.5 \text{ mg L}^{-1}$, organic carbon $< 0.5 \text{ mg L}^{-1}$).

2.2. Photochemical reactions

Photo-Fenton experiments were carried out at the Plataforma Solar de Almería, in a compound parabolic collector solar plant specially developed for photo-Fenton applications [27], able to treat up to 80 L of wastewater. It has a 4.16 m^2 irradiated surface, 44.6 L irradiated volume, and cylindrical UVA-transparent glass tubes with a 46.4 mm internal diameter and 50 mm external diameter. UV radiation was measured by a global UV radiometer (KIPP&ZONEN, model CUV 3) mounted on a platform tilted 37°, which provides data in terms of incident UV (W m^{-2}). This gives an idea of the energy reaching any surface in the same position with regard to the sun. With Eq. (1), combination of the data from several days' experiments and comparison of photoreactors installed at different sites is possible.

$$t_{30W,n} = t_{30W,n-1} + \Delta t_n \frac{\text{UV } V_i}{30 V_T};$$

$$\Delta t_n = t_n - t_{n-1}; \quad t_0 = 0 \quad (n = 1) \quad (1)$$

Table 1
Concentration of alachlor and overall DOC in samples (from photo-Fenton pre-treatment) tested with *P. putida* CECT 324

Sample	1	2	3	4	5	6	7	8	9
t_{30W} (min)	0	34	61	81	91	103	110	122	134
DOC (mg L ⁻¹)	105	98.4	86.7	84.1	78.4	73.1	63.4	54.5	36.7
Alachlor (mg L ⁻¹)	123.4	26	8.62	4.82	1.33	1.36	1.04	1.3	0
Mineralization (%)	0	6	17	20	25	30	40	48	65
Consumed H ₂ O ₂ (mg L ⁻¹)	1.1	3.1	23.1	50.0	91.8	126.9	162.0	207.0	287.0

Consumed H₂O₂ is also included.

where UV is the average solar ultraviolet radiation measured during Δt_n , t_n is the experimental time for each sample, V_T is the total volume of water loaded in the pilot plant (75 L), V_i is the total irradiated volume (44.6 L, glass tubes) and t_{30W} is a “normalized illumination time”, which refers to a constant solar UV power of 30 W m⁻² (typical solar UV power on a sunny day around noon in a Mediterranean country). The temperature inside the reactor was kept at 30 °C by means of a temperature control system consisting of heating elements in the pipes, and a heat exchanger with a secondary cooling water cycle.

For the photo-Fenton reaction, the plant was loaded with 75 L of an aqueous solution of the parent compounds at initial concentrations of 123.4 mg L⁻¹ of alachlor and 103 mg L⁻¹ of pyrimethanil. The pH was adjusted to 2.7–2.9 with H₂SO₄. The Fe²⁺ concentration of 20 mg L⁻¹ had been previously demonstrated not to affect bacterial growth. At the beginning of the process the collectors were covered, the pH was adjusted and ferrous iron salt (FeSO₄·7H₂O) was added. After each addition of reagents, the mixture was recirculated until well homogenised. Finally, the necessary quantity of reagent-grade hydrogen peroxide (30%, w/v) was added. Then the collectors were uncovered and photo-Fenton began (t_{30W} = 0 min). Hydrogen peroxide was measured frequently and consumed reagent was continually replaced in order to keep the concentration at the initial 100 mg L⁻¹. From these data consumed hydrogen peroxide was calculated. Hydrogen peroxide was analysed by iodometric titration, although, since this method is very time consuming (around 45 min), it was also frequently determined in fresh sample solutions using Merckoquant Paper (Merck Cat. No. 1.10011.0001). Hydrogen peroxide present in the samples from photo-Fenton experiments was removed using catalase (2500 U mg⁻¹ bovine liver, 100 mg L⁻¹) acquired from Fluka Chemie AG (Buchs, Switzerland) after adjusting the sample pH to 7.

Table 2
Concentration of pyrimethanil and overall DOC in samples (from photo-Fenton pre-treatment) tested with *P. putida* CECT 324. Consumed H₂O₂ is also included

Sample	1	2	3	4	5	6	7	8	9
t_{30W} (min)	0	98	105	108	111	127	153	187	224
DOC (mg L ⁻¹)	72.1	67	58.4	49.4	40.1	25.4	17.5	13.7	10.2
Pyrimethanil (mg L ⁻¹)	103	23	2.3	0	0	0	0	0	0
Mineralization (%)	0	7	19	32	44	65	76	81	86
Consumed H ₂ O ₂ (mg L ⁻¹)	2.1	44.9	88.0	148	208	263	330	407	480

2.3. Microorganism

P. putida CECT 324 was acquired from the Spanish Type Culture Collection (Colección Española de Cultivos Tipo, Valencia, Spain). Cultures were grown at pH 7.2 in beef extract, 1 g L⁻¹, yeast extract, 2 g L⁻¹, peptone, 5 g L⁻¹, NaCl, 5 g L⁻¹ and agar powder, 15 g L⁻¹, and kept in a cryogenic solution (glycerol 87%) at -70 °C.

2.4. Flask cultures

For parent pesticide biodegradability and toxicity studies, duplicate cultures were incubated at 30 °C on a rotary platform shaker (150 rpm, 2.6 cm stroke) in 100 mL Erlenmeyer flasks filled with 20 mL of different alachlor and pyrimethanil solutions (0, 30, 60, 90 and 120 mg L⁻¹). The flasks were inoculated with 80 µL of the bacterial stock described above previously defrosted at room temperature.

For biodegradability studies of pesticides treated by photo-Fenton, duplicate cultures were incubated at 30 °C on a rotary platform in 250 mL Erlenmeyer flasks filled with 50 mL of culture medium. The flasks were inoculated with 200 µL of bacterial stock. The pesticides (123.4 mg L⁻¹ alachlor and 103 mg L⁻¹ pyrimethanil) treated by photo-Fenton for different periods of time formed an additional carbon source for which biodegradability was going to be evaluated. Initial dissolved organic carbon (DOC) and pesticide concentrations for each sample are shown in Tables 1 and 2. Samples were filtered through 0.20 µm syringe filters (AAWG, 47 mm, Millipore). The pH value was adjusted to 7.0 with NaOH 0.1 N. Inoculum viability was checked with 80 µL of bacterial stock in 100 L Erlenmeyer flasks filled with 20 mL of baseline culture medium described below.

The baseline medium in all flask cultures (beef extract, 3.2 mg L⁻¹, yeast extract, 6.4 mg L⁻¹, peptone, 16 mg L⁻¹, NaCl, 16 mg L⁻¹ glycerol 87% (v/v), 0.8 mL/L, 0.5 g L⁻¹

NH_4Cl , 0.5 g L^{-1} K_2HPO_4 , 0.5 g L^{-1} KH_2PO_4 , 0.5 g L^{-1} $\text{MgSO}_4 \cdot 7\text{H}_2\text{O}$, and 10 mL L^{-1} of trace mineral solution [28]) provides a DOC concentration of approximately 360 mg L^{-1} , considered a biodegradable carbon source. Initial bacterial concentration was 20 mg L^{-1} in all flask cultures.

2.5. Bubble column bioreactor

Fermentation was done at 30°C in a 12 L working-volume bubble column bioreactor with an aspect ratio of 6 and reactor vessel diameter of 0.125 m. Gas was sparged through a perforated plate (1.5 mm hole diameter) located at the base of the reactor. Dissolved oxygen was measured on line using a Crison 60-50 polarographic electrode. Oxygen uptake rate (OUR) was measured during culturing by the method reported by Casas López et al. [29]. The gas flow rate was held constant at 0.83 vvm, giving rise to an overall volumetric oxygen transfer coefficient of 20.5 h^{-1} . It can be assumed that oxygen was not a growth-rate-limiting substrate in the experiments. pH was measured with a pH electrode (Crison 55 33). The reactor was fitted with a temperature control jacket. The top degassing zone of the column had a jacket of its own cooled to 8°C to prevent wall growth. 48 mL of bacteria stock was directly inoculated in the bubble column bioreactor. Initial bacterial concentration was 20 mg L^{-1} . Inoculum viability was checked as described in Section 2.4. Automatic sampling was done by Sigma 900 Portable Sampler. Experiments were performed in duplicate with repeated runs for different times for accurate assessment of variability.

A blank column contained the mineral medium described above and the carbon source supplied by the baseline culture medium. For biodegradation kinetics experiments, alachlor and pyrimethanil were treated by photo-Fenton (30.2 and 27.2% mineralization) as in the Erlenmeyer flask cultures. Therefore, initial DOC was 61.6 and 76.8 mg L^{-1} for alachlor and pyrimethanil, respectively, and that was increased up to 421.6 and 436.8 mg L^{-1} by the baseline medium. Photo-pre-treated samples were handled in the same way as flask cultures.

2.6. Analytical methods

Biomass concentration was measured by optical density (OD) at 600 nm [30] using a spectrophotometer (Unicam, UV 2, Cambridge, UK). The relationship between dry weight and optical density was found to be $X (\text{mg L}^{-1}) = 403.3\text{OD}_{600} - 5.7$, $r^2 = 0.988$.

The pesticide concentration was analysed using reverse-phase liquid chromatography (Shimadzu Lc10, Kyoto, Japan) with a XTerra MS C_{18} column ($150 \text{ mm} \times 4.6 \text{ mm}$, $5 \mu\text{m}$) running with a mobile phase flow rate of 0.5 mL min^{-1} : alachlor ($\text{H}_2\text{O}/\text{acetonitrile}$ 40/60, 225 nm) and pyrimethanil ($\text{H}_2\text{O}/\text{acetonitrile}$ 50/50, 270 nm). Samples were filtered through $0.20 \mu\text{m}$ syringe filters (AAWG, 47 mm, Millipore) to remove bacteria before HPLC injection. Sample injection volume was $20 \mu\text{L}$.

Mineralization was followed by DOC determination in a Shimadzu-V_{CPH} TOC analyser calibrated with standard solutions of potassium phthalate. Samples were pre-filtered through $0.20 \mu\text{m}$ syringe filters (AAWG, 47 mm, Millipore).

3. Results and discussion

3.1. Alachlor degradation

Photo-Fenton degradation of this herbicide has previously been reported in the same experimental device described in Section 2.2, but at an initial concentration of around 50 mg L^{-1} and 2, 10, 20 and 55 mg L^{-1} of Fe^{2+} [10,31]. In all cases, dechlorination was much faster than the disappearance of DOC. When the catalyst concentration was 20 mg L^{-1} , alachlor was completely eliminated during the “dark” Fenton reaction (without sunlight), but without attaining any mineralization. In fact, more than 90% of mineralization was only attained after illumination ($t_{30 \text{ W}} = 20 \text{ min}$) and a H_2O_2 consumption of around 35 mmol L^{-1} , indicating that using low iron concentration the “dark” Fenton was not relevant. Indeed, the consumption of hydrogen peroxide just when photo-Fenton began ($t_{30 \text{ W}} = 0 \text{ min}$) was not relevant (see Table 1). Apart from these kinetic degradation studies, toxicity using *Vibrio fischeri* and biodegradability (with activated sludge, Zahn-Wellens test) analyses at different stages of alachlor oxidation, were also performed previously [27]. We were motivated to continue the study with *P. putida*, as using a well-known compound could help us interpret the results. We also decided to increase initial concentration to almost the solubility limit (123.4 mg L^{-1}) in order to obtain the highest possible concentration of alachlor intermediates before applying *P. putida* treatment.

In the toxicity study, *P. putida* was able to grow on the available degradable carbon source with alachlor in solution. An average DOC consumption of $330 \pm 20.9 \text{ mg L}^{-1}$ was measured at 96 h of culture regardless of pollutant concentration which remained constant at its initial value as determined by HPLC measurement. This shows that *P. putida* growth is not influenced by alachlor concentration. On the contrary, acute toxicity tests with *Vibrio fischeri* showed EC_{50} for alachlor of around 100 mg L^{-1} [4,18].

Different photocatalytic treatment times were applied to the solutions to modify the alachlor chemical structure and transform it into non-toxic and biodegradable intermediates. The remaining carbon was quantified by the DOC due to alachlor and intermediates (Table 1). H_2O_2 consumed during the test is also included in Table 1. At each photo-Fenton treatment time, expressed as $t_{30 \text{ W}}$, biodegradation of intermediates by *P. putida* was assayed in Erlenmeyer flasks as described in Section 2.4. After 96 h of culture, the biodegradation efficiency (E_f) of photoreaction intermediates was calculated as the ratio between the actual organic carbon uptake and maximum DOC consumption [32]. Eq. (2) expresses E_f as a percentage:

$$E_f = \frac{\text{DOC}_i - (\text{DOC}_f - \text{DOC}_m)}{(\text{DOC}_i)} \times 100 \quad (2)$$

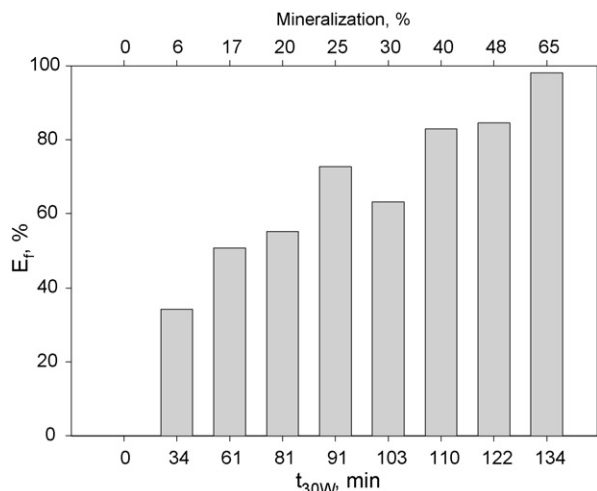


Fig. 1. Biodegradation efficiency (E_f) for alachlor photo-treated samples as a function of t_{30W} and mineralization at 96 h.

where DOC_i is the initial DOC concentration given by photoreaction intermediates, DOC_f is the measured DOC concentration at the end of culture and DOC_m is the minimum concentration that cannot be metabolized by the cells, which is the background level in the blank medium accepted as 30 mg L^{-1} .

Biodegradability of polluted water usually increases with photocatalytic treatment time. Fig. 1 shows the increase in biological treatment efficiency from 34 to 78% and from 6 to 25% mineralization with photo-Fenton reaction time in the alachlor experiments (see Table 1). However DOC biodegradation fell at 103 min. During photo-Fenton, many intermediates are formed from alachlor due to the replacement of hydroxyls, elimination of alkyls, opening of the aromatic ring, etc. [33]. It has been reported that some of these intermediates, mainly aniline derivatives [12], such as the metabolite 2,6-diethylaniline [4], are more toxic than alachlor, so the decrease observed in E_f at $t_{30W} = 103$ min is due to the presence of toxic intermediates. Beyond this time, biological treatment efficiency increased from 63 to 98% at the end of photo-Fenton reaction ($t_{30W} = 134$ min) because of toxic intermediates were then degraded.

At the start of phototreatment, $t_{30W} = 0$, no alachlor intermediates or bacteria growth on the baseline medium had formed. At this point efficiency is zero in agreement with the toxicity studies mentioned above. Nonetheless, *P. putida* was able to biodegrade the intermediates generated, even when parent alachlor is still present at t_{30W} of 34, 61 and 81 min (Fig. 1), although alachlor was not consumed, as confirmed by HPLC measurements. The slight alachlor decrease found in certain cases (i.e., 61 min or higher treatment time) could be attributed to adsorption on biomass.

Results when photo-Fenton mineralization was not as high (around 30%), but alachlor had disappeared were scaled up in a 12 L bubble column bioreactor. Under these conditions, $E_f = 60\%$ and higher efficiency could reasonably be expected as time of photocatalytic treatment increases. It was assumed that longer photo-Fenton treatment times would always enhance water biocompatibility. Therefore, an alachlor solution also containing 123.4 mg L^{-1} was treated by photo-Fenton for 110 min,

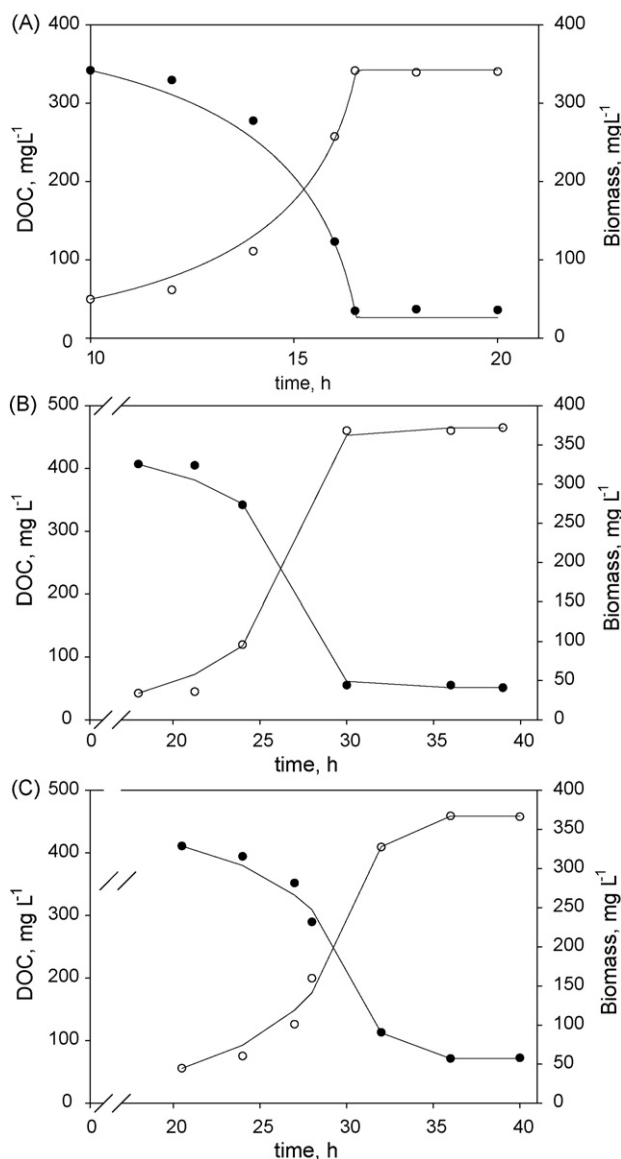


Fig. 2. Biomass growth (○) and DOC consumption (●) in a bubble column bioreactor. (A) Blank, (B) alachlor photo-treated solution and (C) pyrimethanil photo-treated solution solid lines show model estimations.

which mineralized 30.2% (H_2O_2 consumption 4.8 mmol L^{-1}) and decreased the pesticide concentration to 2.4 mg L^{-1} , leaving 61.6 mg L^{-1} DOC for further biological treatment. An additional blank experiment was carried out with the baseline biodegradable carbon source and no pesticide intermediates to compare the kinetics parameters.

Fig. 2 shows the changes in biomass concentration and DOC with culture time for the scaled-up experiment. Once cells had adapted to the treated alachlor solution, they grew in 8 h, causing a sharp decrease in DOC and intense respiration. Likewise, the maximum specific respiration rate, an important design parameter for scale-up, was 13.74 and $11.53 \text{ mmol O}_2 \text{ g}^{-1} \text{ h}^{-1}$ in the blank and treated alachlor culture, respectively.

Fig. 3 shows a decrease in cell metabolic activity caused by photoreaction intermediates, causing a drop in DOC uptake rates from 100 to $80 \text{ mg L}^{-1} \text{ h}^{-1}$ for the blank and alachlor, respec-

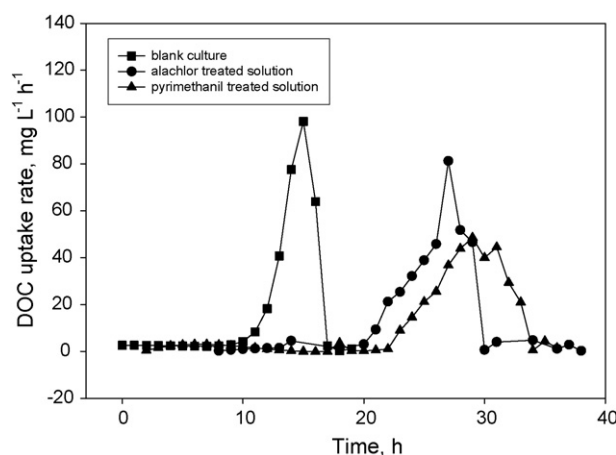


Fig. 3. DOC uptake rate versus culture time in the blank,alachlor and pyrimethanil experiments.

tively. The delay in reaching the maximum DOC uptake rate is longer in the photo-treated sample than in the blank because of changes in the lag phase and growth rate discussed below. Therefore, *P. putida* is sensitive to photo-produced intermediates giving rise to different behaviour: longer lag phases, slower respiration rates and carbon uptake rates.

Kinetics was fitted to Andrews' growth model because of its mathematical simplicity and wide acceptance for representing the growth kinetics of inhibitory substrates [34]:

$$\mu = \frac{\mu_{\max} S}{K_S + S + (S^2/K_I)} \quad (3)$$

where S represents the substrate concentration, in this case the DOC available for consumption by the cells. The constant K_S indicates the ability of microorganisms to grow at low substrate levels and K_I is the inhibition constant. A high K_I indicates that the inhibition effect can be observed only in a high concentration range.

The model below was used for the equations for change in biomass concentration:

$$\frac{dX}{dt} = \mu X \quad (4)$$

and for DOC concentration over time once growth started after lag phase:

$$r_S = \frac{dS}{dt} = -\frac{\mu X}{Y_{X/S}} \quad (5)$$

All model parameters were determined by fitting the proposed differential equations to the experimental data using Matlab™ (ver. 6.5). The Matlab Optimization Toolbox was used to find the model parameters. Constrained nonlinear pro-

gramming was used for the search. The target function to be minimized was defined as a function of the vectorized state space, X_{exp} , that is, all substrate data plus the biomass off-line readings. Note that each state could have a different number of points. Simulation points were picked at the same time as the data and arranged in the same order to conform the vectorized simulated state space vector, X_{mod} . The objective function, J , is then defined as weighted squared differences, as follows:

$$J = \sum_{i=1}^N \left(\frac{X(i)_{\text{exp}} - X(i)_{\text{mod}}}{X(i)_{\text{exp}}} \right)^2 \quad (6)$$

The state vector contains the biomass and substrate data collected following the experimental procedure. The model state vector was sampled at the same times by defining an appropriate time vector to numerically solve the differential equations mentioned above. Upper and lower levels were taken from the literature.

Table 3 gives the model parameter values. The specific growth rate depends on the presence of photo-Fenton degradation products. First, μ_{\max} is lower and K_S is higher than the blank culture showing the minor affinity of cells for growth on the photo-treated medium. Inhibition constants are lower than in initial DOC concentrations (around $\sim 100 \text{ mg L}^{-1}$ for K_I versus $\sim 400 \text{ mg L}^{-1}$ for organic carbon) indicating that inhibition phenomena must be taken into account even for the baseline medium.

Calculated specific growth rates for the blank and for the photo-treated solution are 0.30 and 0.23 h^{-1} , respectively, at the culture time when carbon uptake rates are maximum, giving:

$$\frac{\mu_{\text{Blank}}}{\mu_{\text{Alachlor}}} = \frac{0.30}{0.23} \approx \frac{r_{S, \text{Blank}}}{r_{S, \text{Alachlor}}} = \frac{100}{80} \approx \frac{r_{O_2, \text{Blank}}}{r_{O_2, \text{Alachlor}}} = \frac{13.74}{11.53} \quad (7)$$

As each rate was determined independently, Eq. (7) shows the fit of the growth model, which had a mean ratio of 1.25 ± 0.05 .

Biodegradation efficiency (E_f) of the photoreaction intermediates as expressed by Eq. (2) was 56.8% in Erlenmeyer flask at 103 min (see Fig. 1) in 96 h. The main difference in scaled-up experiment is not the efficiency (65.8%) but the 30 h required to achieve it. Therefore, for qualitative results (i.e., for determining whether the photo-treated solutions could be biocompatible for biomass growth), experiments in flasks might be recommendable, but not for adequate quantification of biomass growth or DOC uptake, key parameters for proper biotreatment design.

Table 3
Model growth kinetics parameter values

	Maximum specific growth rate, μ_{\max} (h^{-1})	Saturation constant, K_S (mg L^{-1})	Inhibition constant, K_I (mg L^{-1})
Blank	0.83	1.75	115
Alachlor	0.71	55.2	112
Pyrimethanil	0.59	55	110

3.2. Pyrimethanil degradation

As in the case of alachlor, photo-Fenton degradation ($20 \text{ mg L}^{-1} \text{ Fe}$) of this pesticide has been studied previously [9], concluding that 50 mg L^{-1} of the parent compound was almost eliminated during the Fenton reaction (without sunlight), and 80% of the initial DOC was successfully mineralized consuming around 45 mmol L^{-1} of H_2O_2 . Pyrimethanil was completely eliminated during the “dark” Fenton reaction (without sunlight), but without attaining any mineralization, indicating that also in this case the “dark” Fenton was not relevant. Consumption of hydrogen peroxide at $t_{30\text{W}} = 0 \text{ min}$ included in Table 2 corroborates this statement. Toxicity using *Vibrio fischeri* at different treatment stages was also evaluated, demonstrating that toxicity decreased during the photo-Fenton treatment. The formation of relative stable aliphatic intermediates (acetylurea, acetamide and formamide) after opening of the pyrimidine ring during the photo-treatment has also been detected by other researchers [8]. This effect keeps the nitrogen mass balance from being closed, and maintains the DOC concentration relatively high up to the end of the process (9 mg L^{-1}). For the same reasons as for alachlor, we chose a well-known compound but at a higher initial concentration than in previous studies.

In the pyrimethanil toxicity study, DOC consumption was similar to alachlor, $333.6 \pm 14.3 \text{ mg L}^{-1}$ although in 144 h of culture instead of 96 h. This delay is in agreement with other pyrimethanil studies that show an EC_{50} of 36.1 mg L^{-1} [9] compared to the 100 mg L^{-1} reported for alachlor (Section 3.1). Indeed, as in the alachlor experiment, pyrimethanil was not consumed by *P. putida*.

Intermediates generated in photo-Fenton-treated pyrimethanil solutions are more biodegradable than the parent compound (Fig. 4). Agüera et al. [8] observed in a study of degradation of pyrimethanil that although many transient species were formed during the process, they were not toxic to *Vibrio fischeri* and a continuous decrease was observed in the percentage of inhibition. Up to 105 min of $t_{30\text{W}}$, biodegrad-

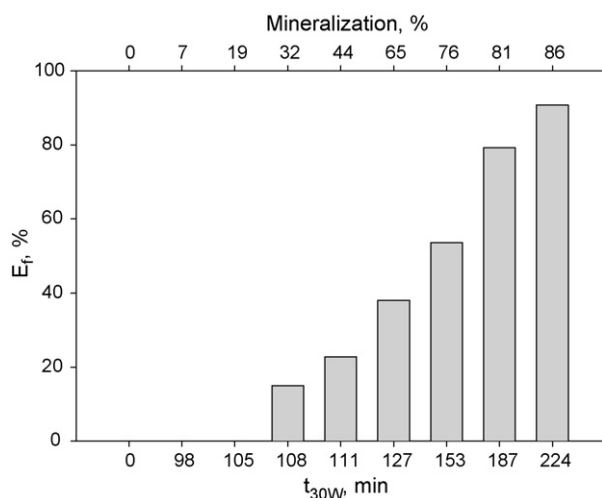


Fig. 4. Biodegradation efficiency (E_f) for pyrimethanil photo-treated samples as a function of $t_{30\text{W}}$ and mineralization at 144 h.

ability efficiency was negligible (as shown in Fig. 4) and at 108 min (32% mineralization) efficiency was only 15%. Beyond this photo-treatment intensity, efficiency increased up to its maximum of 91% at $t_{30\text{W}} = 224 \text{ min}$. Compared to the alachlor experiment, longer photocatalytic treatment times are required to reach equivalent efficiencies and total disappearance of the pure substance is required for biodegradation of intermediates formed. As confirmed by HPLC measurements, pyrimethanil was not biodegraded at 0, 98 and 105 min of treatment time.

For kinetics estimations, a pyrimethanil solution was pre-treated by photocatalysis to 27.2% mineralization, the minimum photo-Fenton treatment time to reach biodegradability. As shown in Table 2 and Fig. 4, biodegradability was enhanced only after 32% mineralization. It was not possible to reach exactly the same point in consecutive runs (32 and 27.2%, respectively) but a slight difference in mineralization should not influence overall results, as demonstrated below.

Growth took place in 16 h once cells adapted to the pyrimethanil-treated solution. The maximum specific respiration rate ($7.34 \text{ mmol O}_2 \text{ g}^{-1} \text{ h}^{-1}$) and DOC uptake rate ($50 \text{ mg L}^{-1} \text{ h}^{-1}$; Fig. 3) were lower than for the photo-degraded alachlor solution.

Data fit to Eq. (3) for the pyrimethanil-treated solution as shown in Fig. 2C gave the parameter values presented in Table 3. The lower μ_{max} is in agreement with the longer growth period (16 h) observed in Fig. 2C, while there was no difference in K_S and K_I with regard to the photo-treated alachlor solution. Yield coefficient on substrate ($Y_{X/S}$) was 0.94 for alachlor and pyrimethanil experiments.

Analogous to Eq. (7), the rates calculated for the blank and photo-treated pyrimethanil solution are:

$$\frac{\mu_{\text{Blank}}}{\mu_{\text{Pyrimethanil}}} = \frac{0.30}{0.18} \approx \frac{r_{S, \text{Blank}}}{r_{S, \text{Pyrimethanil}}} = \frac{100}{50} \approx \frac{r_{\text{O}_2, \text{Blank}}}{r_{\text{O}_2, \text{Pyrimethanil}}} = \frac{13.74}{7.34} \approx 1.85 \pm 0.16 \quad (8)$$

On the other hand, biodegradation efficiency (E_f) of the pyrimethanil photoreaction intermediates was 44.8%, three times higher than in the Erlenmeyer flask at a $t_{30\text{W}}$ of 108 min (15%) and in a shorter culture time of 32 h. Therefore, culture conditions have an impact on biodegradation results that must be kept in mind when considering biodegradability of a test substance. The same considerations concerning scaled up tests for biotreatment design included at the end of Section 3.1 should be taken into account in this case.

4. Concluding remarks

Neither alachlor nor pyrimethanil are toxic to *P. putida* CECT 324 at the test concentrations, but they are not biodegradable. Therefore, *P. putida* is useful for determining biodegradability enhancement of wastewater containing pesticides by an AOP. A $\sim 100 \text{ min}$ photo-Fenton pre-treatment was efficient enough to enhance biodegradability, with the biological oxidation response dependent on the pesticide tested. The different respiration and

carbon uptake rates found for alachlor and pyrimethanil pre-treated solutions are related to a change in the growth kinetics of the model microorganism. It has been demonstrated that by proper selection of the photo-Fenton pre-treatment time, the wastewater could be rendered biodegradable and that *P. putida* could be used to determine this time. Moreover, as it is a pure strain, results would be reproducible, which is not often possible with activated sludge.

References

- [1] United Nations, Report of the World Summit on Sustainable Development, Johannesburg, South Africa, 26 August–4 September 2002.
- [2] European Commission, Directive 2000/60/EC of the European Parliament and of The Council of 23 October 2000 establishing a framework for Community action in the field of water policy, Off. J. Eur. Communities (2000) L 327/1.
- [3] G. Horberg, Risk, science and politics, Alachlor regulation in Canada and the United States, Can. J. Polit. Sci. 23 (2) (1990) 257–277.
- [4] O. Osano, W. Admiraala, H.J.C. Klamerc, D. Pastorc, E.A.J. Bleekera, Comparative toxic and genotoxic effects of chloroacetanilides, formamidines and their degradation products on *Vibrio fischeri* and *Chironomus riparius*, Environ. Pollut. 119 (2002) 195–202.
- [5] G. Grizard, L. Ouchchane, H. Roddier, C. Artonne, B. Sion, M.-P. Vasson, L. Janny, *In vitro* alachlor effects on reactive oxygen species generation, motility patterns and apoptosis markers in human spermatozoa, Reprod. Toxicol. 23 (2007) 55–62.
- [6] European Food Safety Authority (EFSA), Conclusion on the peer review of Pyrimethanil, Sci. Rep. 61 (2006) 1–70.
- [7] G.A. Peñuela, D. Barceló, Comparative degradation kinetics of alachlor in water by photocatalysis with FeCl₃, TiO₂ and photolysis, studied by solid phase disk extraction followed by gas chromatographic techniques, J. Chromatogr. A 754 (1996) 187–195.
- [8] A. Agüera, E. Almansa, A. Tejedor, A. Fernandez-Alba, Photocatalytic pilot scale degradation study of pyrimethanil and of its main degradation products in waters by means of solid-phase extraction followed by gas and liquid chromatography with mass spectrometry detection, Environ. Sci. Technol. 34 (2000) 1563–1571.
- [9] I. Oller, W. Gernjak, M.I. Maldonado, L.A. Perez-Estrada, J.A. Sanchez-Perez, S. Malato, Solar photocatalytic degradation of some hazardous water-soluble pesticides at pilot-plant scale, J. Hazard. Mater. B138 (2006) 507–517.
- [10] M.I. Maldonado, P.C. Passarinho, I. Oller, W. Gernjak, P. Fernández, J. Blanco, S. Malato, Photocatalytic degradation of EU priority substances: a comparison between TiO₂ and photo-Fenton in a solar pilot plant, J. Photochem. Photobiol. A: Chem. 185 (2007) 354–363.
- [11] S. Parra, V. Sarria, S. Malato, P. Péringier, C. Pulgarin, Photochemical versus coupled photochemical–biological flow system for the treatment of two biorecalcitrant herbicides: metobromuron and isoproturon, Appl. Catal. B: Environ. 27 (2000) 153–168.
- [12] M.J. Farré, M.I. Franch, S. Malato, J.A. Ayllón, J. Peral, X. Doménech, Degradation of some biorecalcitrant pesticides by homogeneous and heterogeneous photocatalytic ozonation, Chemosphere 58 (2005) 1127–1133.
- [13] S. Malato, J. Blanco, M.I. Maldonado, P. Fernández, W. Gernjak, I. Oller, Treatment of chlorinated solvents by TiO₂ photocatalysis and photo-Fenton: influence of operating conditions in a solar pilot plant, Chemosphere 58 (2005) 391–398.
- [14] M. Bressan, L. Liberatorre, N. D'Alessandro, L. Tonucci, C. Belli, G. Ranalli, Improved combined chemical and biological treatments of olive oil mill wastewaters, J. Agric. Food Chem. 52 (2004) 1228–1233.
- [15] A.E. Da Hora Machado, T.P. Xavier, D.R. de Souza, J.A. de Miranda, E.T.F. Mendonsa-Duarte, R. Ruggiero, L. de Oliveira, C. Sattler, Solar photo-Fenton treatment of chip board production waste water, Sol. Energy 77 (2005) 583–589.
- [16] C. Pulgarín, M. Invernizzi, S. Parra, V. Sarria, R. Polaina, P. Péringier, Strategy for the coupling of photochemical and biological flow reactions useful in mineralization of biorecalcitrant industrial pollutants, Catal. Today 54 (1999) 341–352.
- [17] V. Sarria, S. Parra, N. Adler, P. Péringier, Recent developments in the coupling of photoassisted and aerobic biological processes for the treatment of biorecalcitrant compounds, Catal. Today 76 (2002) 301–315.
- [18] M. Lapertot, S. Ebrahimi, S. Dazio, A. Rubinelli, C. Pulgarin, Photo-Fenton and biological integrated process for degradation of a mixture of pesticides, J. Photochem. Photobiol. A: Chem. 186 (2007) 34–40.
- [19] D. Suryaman, K. Hasegawa, S. Kagaya, Combined biological and photocatalytic treatment for the mineralization of phenol in water, Chemosphere 65 (2006) 2502–2506.
- [20] E. Evgenidou, I. Konstantinou, K. Fytianos, T. Albanis, Study of the removal of dichlorvos and dimethoate in a titanium dioxide mediated photocatalytic process through the examination of intermediates and the reaction mechanism, J. Hazard. Mater. B 137 (2006) 1056–1064.
- [21] A. Arques, A.M. Amat, A. García-Ripoll, R. Vicente, Detoxification and/or increase of the biodegradability of aqueous solutions of pesticides by means of solar photocatalysis, J. Hazard. Mater. 146 (2007) 447–452.
- [22] D. Mantzavinos, E. Psillakis, Enhancement of biodegradability of industrial wastewaters by chemical oxidation pre-treatment, J. Chem. Technol. Biotechnol. 79 (2004) 431–454.
- [23] P.R. Gogate, A.B. Pandit, A review of comparative technologies for wastewater treatment. II. Hybrid methods, Adv. Environ. Res. 8 (2004) 553–597.
- [24] J. Wiszniewski, D. Robert, J. Surmacz-Gorska, K. Miksch, J.V. Weber, Landfill leachate treatment methods: a review, Environ. Chem. Lett. 4 (2006) 51–61.
- [25] D.F. Ollis, On the need for engineering models of integrated chemical and biological oxidation of wastewaters, Water Sci. Technol. 44 (2001) 117–123.
- [26] M.M. Ballesteros Martín, J.A. Sánchez Pérez, F.G. Ación Fernández, J.L. García Sánchez, J.L. Casas López, S. Malato Rodríguez, A kinetics study on the biodegradation of synthetic wastewater simulating effluent from an advanced oxidation process using *Pseudomonas putida* CECT 324, J. Hazard. Mater., in press.
- [27] M. Lapertot, C. Pulgarín, P. Fernández-Ibañez, M.I. Maldonado, L. Pérez-Estrada, I. Oller, W. Gernjak, S. Malato, Enhancing biodegradability of priority substances (pesticides) by solar photo-Fenton, Water Res. 40 (2006) 1086–1094.
- [28] H. Shim, E. Shin, S.T. Yang, A continuous fibrous-bed bioreactor for BTEX biodegradation by a co-culture of *Pseudomonas putida* and *Pseudomonas fluorescens*, Adv. Environ. Res. 7 (2002) 203–216.
- [29] J.L. Casas López, E.M. Rodríguez Porcel, I. Oller Alberola, M.M. Ballesteros Martín, J.A. Sánchez Pérez, J.M. Fernández Sevilla, Y. Chisti, Simultaneous determination of oxygen consumption rate and volumetric oxygen transfer coefficient in pneumatically agitated bioreactors, Ind. Eng. Chem. Res. 45 (2006) 1167–1171.
- [30] S.J. Wang, K.C. Loh, Modeling the role metabolic intermediates in kinetics of phenol biodegradation, Enzyme Microbial. Technol. 25 (1999) 177–184.
- [31] W. Gernjak, M. Fuerhacker, P. Fernández-Ibañez, J. Blanco, S. Malato, Solar photo-Fenton treatment—process parameters and process control, Appl. Catal. B: Environ. 64 (2006) 121–130.
- [32] M.M. Ballesteros Martín, J.A. Sánchez Pérez, F.G. Ación Fernández, J.L. Casas López, A.M. García-Ripoll, A.M. Amat, I. Oller, S. Malato Rodríguez, Degradation of a commercial pesticide mixture by combined photo-Fenton and *Pseudomonas putida* biological oxidation, Chemosphere, in press.
- [33] H. Katsumata, S. Kaneco, T. Suzuki, K. Ohta, Y. Yobiko, Photo-Fenton degradation of alachlor in the presence of citrate solution, J. Photochem. Photobiol. A: Chem. 180 (2006) 38–45.
- [34] J.F. Andrews, A mathematical model for the continuous culture of microorganisms utilizing inhibitory substrates, Biotechnol. Bioeng. 10 (1968) 707–723.